



**UNIVERSITA' DEGLI STUDI DI**

**PADOVA**

**DIPARTIMENTO DI SCIENZE**

**CHIMICHE**

**CORSO DI LAUREA IN CHIMICA**

“Light-Driven Synthesis and Functionalisation of Bicyclopentanes  
(BCPs)”

**Relatore:** Prof. Luca Dell'amico

**Laureando:** Giacomo Cassarà  
N° 2000310

Anno Accademico 2022/2023



# Index

<b>1 Introduction</b> .....	5
<b>1.1 Benzene bioisosteres</b> .....	5
<b>1.2 <i>Ortho</i>- substituted benzene: bicyclo[2.1.1]hexane (BCHex)</b> .....	5
<b>1.3 <i>Meta</i>- substituted benzene: bicyclo[3.1.1]heptane (BCHep)</b> .....	6
<b>1.4 <i>Para</i>- substituted benzene: bicyclo[1.1.1]pentane (BCP)</b> .....	7
<b>1.5 Aim of the thesis</b> .....	9
<b>2 Structure and reactivity of [1.1.1]propellane:</b> .....	9
<b>3 Synthesis</b> .....	11
<b>3.1 The synthesis of [1.1.1]propellane and secondary production of staffane</b> .....	11
<b>3.2 Photocatalysis</b> .....	12
<b>3.2.1 Photo-induced electron transfer (PET) catalysis</b> .....	12
<b>3.2.2 Proton-coupled electron transfer (PCET) catalysis</b> .....	12
<b>3.2.3 Hydrogen atom transfer (HAT) catalysis</b> .....	12
<b>3.2.4 Atom transfer radical addition (ATRA) process</b> .....	12
<b>4 Triethylborane-initiated reaction</b> .....	13
<b>4.1 Mechanism</b> .....	13
<b>5 Iridium photocatalyzed reaction</b> .....	14
<b>5.1 Mechanism</b> .....	15
<b>6 Organophotocatalyzed reactions</b> .....	16
<b>6.1 EDA Complex</b> .....	16
<b>6.2 An hybrid bioisoster</b> .....	17
<b>6.3 Synthesis of difluoroalkyl BCP <i>via</i> ATRA</b> .....	18
<b>6.3.1 Mechanism</b> .....	18
<b>6.3.2 Organophotocatalyst evaluation</b> .....	19
<b>6.3.3 12ADBA in-depth analysis</b> .....	20
<b>6.4 Synthesis of aryl difluoromethyl BCP</b> .....	21
<b>6.4.1 Mechanism</b> .....	22
<b>6.4.2 Organophotocatalyst evaluation</b> .....	23
<b>7 Conclusions</b> .....	23
<b>8 Bibliography</b> .....	24



# 1 Introduction

## 1.1 Benzene bioisosteres

The benzene ring is one of the most diffused component of pharmaceuticals, in fact it is contained in more than 500 FDA approved drugs. Due to its unique structure and properties, it has a key role in the design of new molecules, often used as scaffold for the active sites. Given these information it does not surprise that chemists in last 50 years have been looking to replace the benzene ring to obtain patent-free molecules with an improved biological activity and physico-chemical profile. This research brought to light 3D saturated compounds. In the next three paragraphs *ortho*, *meta* and *para* benzene bioisosteres will be described and their replacement in biological substrates will be evaluated.

## 1.2 *Ortho*-substituted benzene: bicyclo[2.1.1]hexane (BCHex)

Because of lacking rational design and synthetic methods, *ortho*-benzene's bioisosteres weren't known until 2020, when finally Mykhailiu and coworkers reported a synthesis of BCHex from propellane. It is notable to say that a correct replacement of benzene with saturated bioisosteres is possible only if its function is that of a spacer between two specific substituents, presence of  $\pi$  – protein interactions like cation- $\pi$ ,  $\pi$ - $\pi$  and dipole- $\pi$  would make useless its employment. BCHex has similar size to that of the benzene, although being respectively 3D and 2D shapes, the substituents are conformationally restricted by the bicyclic structure and therefore fixed and DFT calculations showed C-C distance to be similar: 3.3–3.6 Å in BCHex and 3.1 Å in *ortho*-benzene. These three criteria classifies BCHex as an attractive bioisostere.

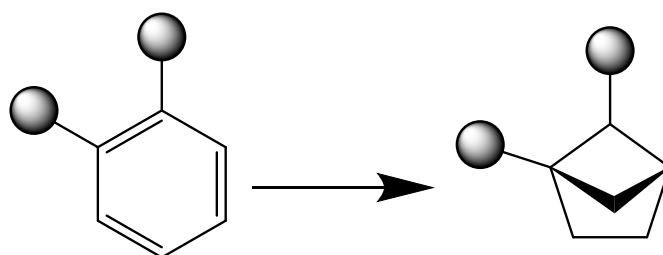


Figure 1. Structure comparison between bicyclo[2.1.1]hexane and *ortho*-substituted benzene.

Crystallographic analysis compared the geometric parameters, using an exit vector plots tool, between BCHex, *Valsartan* and *Telmisartan*, two ipertensive drugs containing benzene ring, those X-ray data were available. Elaborated datas showed the C-variation points r distance to be 0.2Å longer in BCHex, the two plane angles  $\Phi_1$  and  $\Phi_2$  between  $n_1$ ,  $n_2$  (vector used to represent substituents) and the molecule plane were similar. The planarity, as mention before, is different between the two compounds but despite that they are overall alike. Physico-chemical properties were also explored, using a model compound. As for other saturated bioisostere the water solubility increased, from 397  $\mu\text{M}$  to 492  $\mu\text{M}$ , but lipophilicity, measured as logD, remained the same (3.5 in original compound vs 3.7 in the bioisostere). In the end biological activity was studied in *Boscalid* and *Fluxapyroxad*, two fungicides; their BCHex analogues shows the same inhibition of the growth of *Fusarium oxysporum* Schltdl.<sup>1</sup>

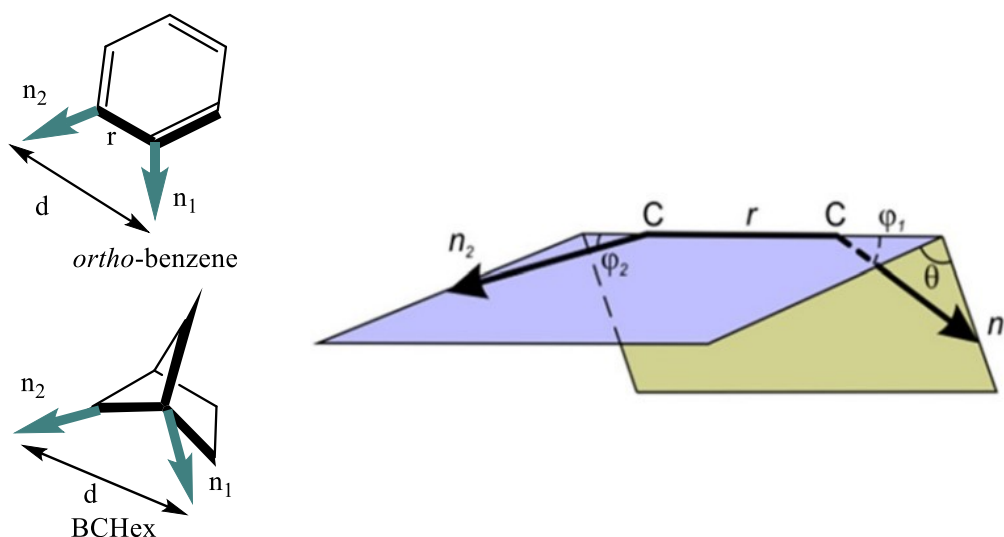


Figure 2. Geometric representation of BCHex and ortho-substituted benzene

### 1.3 *Meta*- substituted benzene: bicyclo[3.1.1]heptane (BCHeP)

Meta-substituted benzenes always have been the most difficult type of benzene to substitute among all three of the meta, ortho and para benzenes due to the difficult synthesis of saturated bioisostere that replicate precisely substituent's vectors. The use of BCHeP can solve this problem and it can be synthesized from [3.1.1]propellane, analogue of [1.1.1]propellane. X-ray analysis permitted to study the vector angles in the BCHeP and in the meta-substituted benzene: the exit vector angles  $\alpha$  had 0-7° difference between each others and the the out-of-plane vector angle  $\phi$  had 3-11°. These low differences consolidate the choice of using BCHeP to retain the original geometry. Besides confirming a general resemblance between the two structures, computational conformer sampling analyzed an additional parameter: the rotational orientation of the planes between substituents groups. The potential energy profile for rotation around C-C bond BCHeP -substituent was calculated to be low, indicating that might show an adaptive conformation that could be useful to link more easily with protein targets. Physicochemical and pharmacological investigations reported similar clogP, topological polar surface area and solubility. BCHeP showed better metabolic stability in human and mouse liver microsomes, also membrane permeability was improved. All these data consolidate the choice to replace *meta*-substituted benzene with BCHeP, making it a very valid bioisostere.<sup>2</sup>

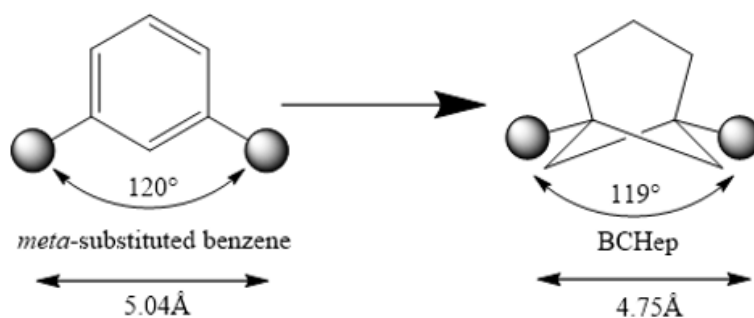


Figure 3. Comparison of distance between substituents: BCHeP and meta-substituted benzene

#### 1.4 *Para*- substituted benzene: bicyclo[1.1.1]pentane (BCP)

Until now three molecules have been used to replace *para*-substituted benzene: BCP, cubane and bicyclo[2.2.2]octane. Auberson, Brocklehurst and Furegati reported a comparison between these compounds based on C-C distances, the none-specific binding and their solubility in water. The distance between connecting atoms is similar in cubane, bicyclo[2.2.2] octane and benzene (2.60Å vs 2.72Å vs 2.82Å), while in BCP is 35% smaller (1.85 Å). Both cubane and BCP show improved solubility and decreased none-specific binding, the second showing 50 times the solubility of benzene. Bicyclo[2.2.2]octane did not show the same improvements and so it's consider a less valuable bioisostere. The use of saturated bioisosteres increases the metabolic stability, in fact aliphatic linkers aren't degraded as benzene derivates do, phenol and aniline for example are fast oxidized *in vivo* by cytochrome-p450. The improved solubility in cubane and BCP is due to the lack of  $\pi$ -stacking between aromatic rings. The behavior of benzene bioisosteres isn't easy to predict but it can be generalized in two scenarios: in the first one where the benzene acts exclusively as a rigid scaffold maintaining the right distance between two substituents; in the second one where the benzene also interacts with proteins via cation- $\pi$  interactions between the phenyl ring and protonated aminoacids;  $\pi$ - $\pi$  interactions between the phenyl ring and the aromatic residue of aminoacids and other weak dipole- $\pi$  interactions. Having BCP shorter C-C bonds than benzene, the pharmacological activity would probably vary, showing even an improvements if the new structure fits better in the receptor binding pocket.<sup>3</sup>

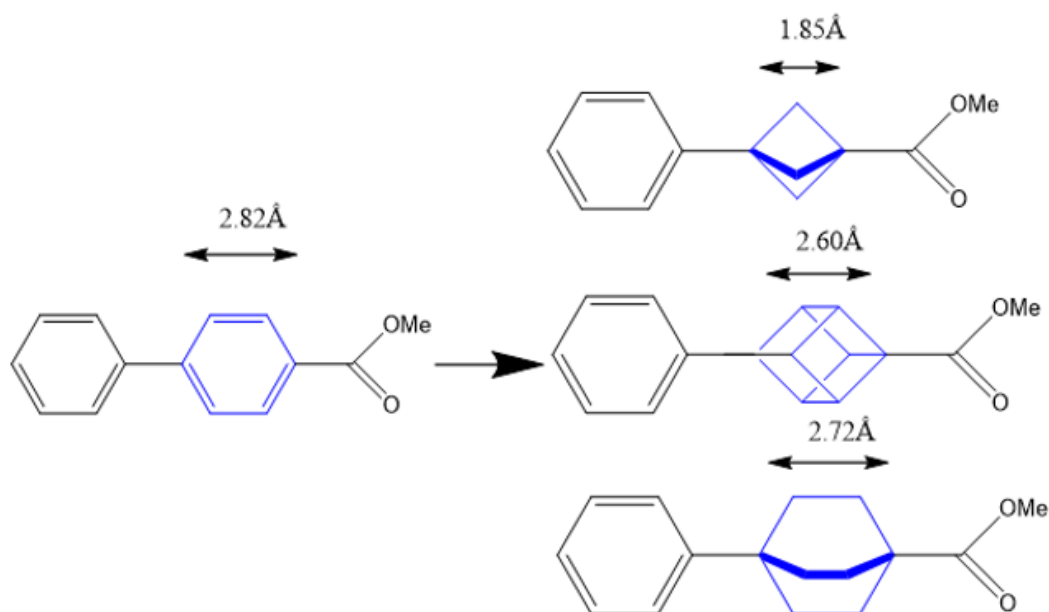


Figure 4. Substituents distance comparison between BCP, bicyclo[2.2.2]octane, cubane and meta-substituted benzene

One important example of bioisosteric replacement is that of  $\gamma$ -secretase inhibitor.  $\gamma$ -Secretase is the enzyme that catalyzes the release of  $\beta$ -amiloids in plasma and in cerebrospinal fluid, these  $\beta$ -amiloids are peptide fragments that aggregates forming oligomers and plaques that genetic and experimental evidences found to be plausible contributors to the Alzheimer's disease development. These compounds are still under development but some as BMS-708,163 have progressed in advanced

clinical trials. The BMS-708,163 bioisostere showed similar potency *in vitro*,  $IC_{50}$  are in fact 0.178 nM for BCP and 0.225 nM for the original compound, leading to the conclusion that fluorophenyl's function is that of a spacer. X-ray confirmed that they orient the functional groups in the same coplanar orientation. Both kinetic and thermodynamic solubility improved (from 0.60 and 1.70  $\mu$ M to 216 and 19.7 $\mu$ M respectively) and there was significant increase of *in vitro* permeability. Great resistance was shown towards metabolic turnover in cryopreserved human hepatocytes (apparent intrinsic clearance ( $CL_{int,app}$ ) < 3.8  $\mu$ L/min/million cells in the bioisostere and  $CL_{int,app}$  = 15  $\mu$ L/min/million cells in the original compound) and similar metabolic stability in human liver microsomes (HLM  $CL_{int,app}$  < 8.17 mL/min/kg in the bioisostere and HLM  $CL_{int,app}$  < 16.2 mL/min/kg in the original compound). The lower value of  $CL_{int,app}$  in cryopreserved human hepatocytes is probably due to the lower lipophilicity of BCP. To guarantee that the use of BCP as bioisostere is the best choice, other alkyl and cycloalkyl compounds were used to replace the fluorophenyl ring in BMS-708,163 but inhibitory potency, metabolic stability, and passive permeability didn't improved enough to justify their use, as a result BCP was the best option. *In vivo* studies on mice highlighted higher concentration of the bioisostere in plasma, brain and cerebrospinal fluid after administering the same dose of the two drugs. Important decrease of  $\beta$ -amyloids after the soministration were registered. These data are respectively good pharmacokinetic and pharmacodynamic aspects.<sup>4</sup>

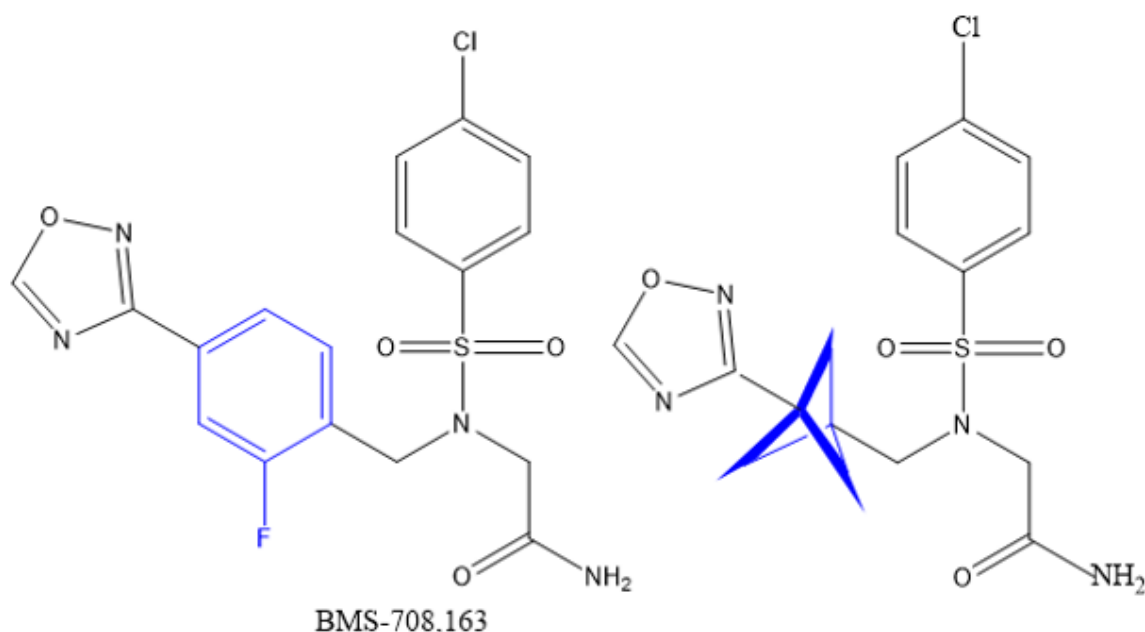


Figure 5. Structure of BMS-708,163 and its BCP bioisostere



## 1.5 Aim of the thesis

The purpose of this thesis is to investigate and elucidate recent synthetic methods of para-benzene analogues: BCPs. This purpose will be briefly discussed introducing theoretical concepts behind the “omniphilic” reactivity of propellane and the formation of electron-donor-acceptor (EDA) complexes. An eye will be kept on mechanisms and photocatalyst, deepening their principal aspects.

## 2 Structure and reactivity of [1.1.1]propellane:

All the synthesis of BCPs begin with the shell-opening of [1.1.1]propellane, in this paragraph we will cover the structure and reactivity of this fundamental precursor.

Propellane is a strained molecule, that means it has distorted bond length, bond angles and torsional variations compared to classical carbon-carbon bonds. Consequently, its radical attack by the intermediate III is a strain release reaction. This difference between classical and strained compounds is better highlighted by the measure of the strain energy, which is the difference between the found heat of formation ( $\Delta H_f$ ) and that expected for a strain-free molecule with the same number of atoms, this criteria also help us building a scale on which we can better classify different strained compounds.<sup>5</sup> [1.1.1]Propellane has a total strain energy between 98 and 113 kcal mol<sup>-1</sup> but only 30kcal mol<sup>-1</sup> comes from the cleavage of the C1-C3 bond. Other molecules, such as cyclopropane, undergo ring-opening reactions thanks to strain-energy relieve but do not possess the high reactivity with both nucleophiles, electrophiles and radicals, wich propellane seems to have. These evidences suggest that other factors might influence his reactivity. DFT studies and in-depth theoretical analysis demonstrate that change in electron delocalization over the carbon structure defines the observed chemistry. Propellane has an unique structure, in particular its C1-C3 bond forces an inverted tetrahedral geometry. Studies have proposed it to be best described as a charge-shift bond, whose stability is due to resonance stabilization between the covalent structures. This type of bonding emerge from Pauli repulsion between C1-C3 and C1/3-C2 linkages. Electron density delocalization from the C1-C3  $\sigma$  orbitals to  $\sigma^*$  orbitals reduces the high electronic repulsion inside the propellane cage; also charge is depleted from the center of the structure (red lobes in figure 11) and delocalized onto the central carbon atoms (blue lobes in figure 11). This two effects combined can be considered as a  $\sigma$ - $\pi$  delocalization  $\sigma_{C1-C3} \rightarrow [ \sigma_{C1-C3}^* + \pi ]$ , where electrons from the C1-C3  $\sigma$  MO partially populate the C1-C3  $\sigma^*$  MO, which possess the correct symmetry to overlap with the p system formed from p orbitals on the central carbon atoms. This ground state structure relieves Pauli repulsion inside the propellane cage, moreover its pliable electron density is the reason why propellane can react with

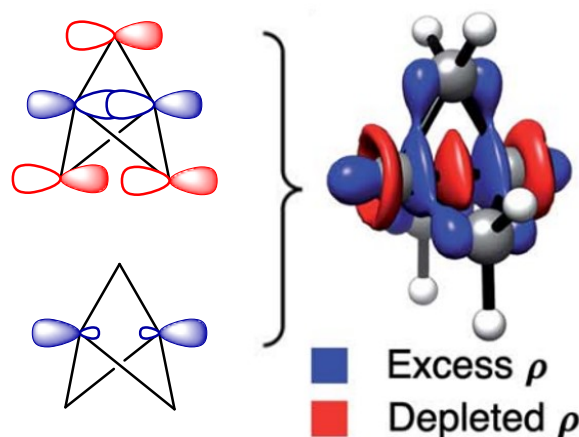


Figure 6. Representation of [CASSCF(2,2)]-[RHF] electron density difference of propellane<sup>6</sup>

both electron-rich, electron deficient and radical species, giving the impression to be an “omniphilic” molecule.<sup>6</sup>

Theoretical studies also deepened the types of reactions which propellane can undergo and found out that anionic and radical additions increases the electronic repulsion inside the carbon structure, which is already electron-rich, causing a barrier to addition. To counterbalance this effect, after the transition state occurs, stabilization through  $\sigma$ - $\pi$  delocalization of electron density over the carbon structure takes place and to maximize the stabilization, the structure gets compressed.

Electrophilic attacks involve the transfer of electron density from an electron-rich structure to a cation. This process occurs without a significant energy barrier because the reduction of Pauli repulsion between C1–C3 and C1/3–C2 linkages, facilitates the transfer of electrons. However, it's important to understand that the stability of the propellane cage structure is maintained by the  $\sigma$ - $\pi$  delocalization, which arises from the Pauli repulsion. It follows that when Pauli repulsion is lost, the stability is compromised or lost and it leads to spontaneous fragmentation of the structure, resulting in the formation of a bicyclo[1.1.0]butyl-1-carbinyl cation. In essence, the loss of electron density can trigger this kind of fragmentation reaction. The presence of substituent in central carbon atoms in the propellane structure can alter the degree of  $\sigma$ - $\pi$  delocalization, influencing both its ground state stability and its reactivity. In this case both electronegativity and the ability to delocalize electron density will have a role<sup>6</sup>.

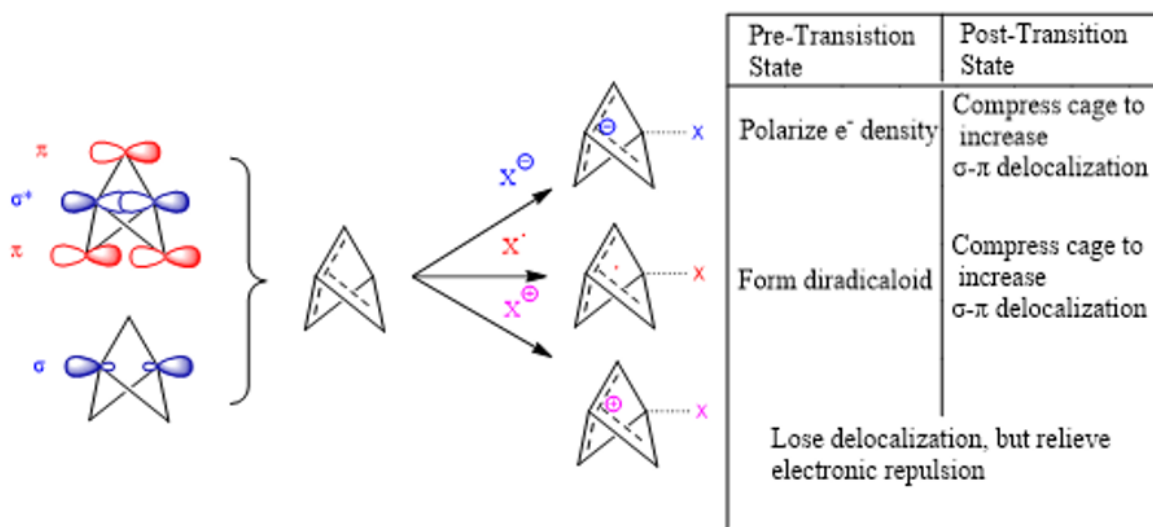


Figure 7. Reactivity of [1.1.1]propellane with change in the electron density distribution over the structure

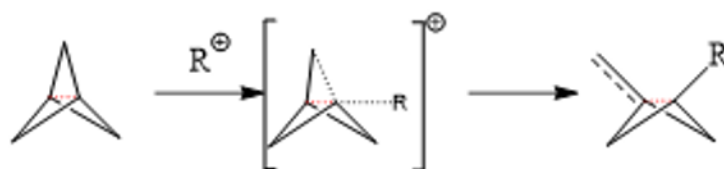


Figure 8. Formation of bicyclo[1.1.0]butyl-1-carbinyl cation

### 3 Synthesis

After viewing the importance of BCPs in pharmaceuticals, it is now important to cover its synthesis and functionalization. In the past it could only be achieved using harsh conditions such as highly activated reagents<sup>7</sup>, mercury lamp irradiation of alkyl and aryl halides<sup>8</sup> or methyllithium-promoted alkyl halide addition<sup>9</sup>. These methods had limited functional group compatibility or scalability and therefore slowed down the wide synthesis and installation of BCPs in known compounds, despite the already covered benefits it could have brought. Radical strain-release reactions carried out under photocatalytic conditions is a convenient option, principal advantages are: an expansive driving force arising from the release of strain; the existence of open-shell intermediates, useful for their high reactivity; the formation of rigid three-dimensional products, which can be challenging or impossible to produce through ionic reactions; the use of mild reaction conditions that reduce the risk of product decomposition and incompatibility with functional groups<sup>5</sup>. Modern synthetic methods use radical chain reactions started by triethyl borane initiators or photocatalyzed radical reactions in presence of transition metals or organic catalysts. In this chapter these strategies will be explored.

#### 3.1 The synthesis of [1.1.1]propellane and secondary production of staffane

The [1.1.1]propellane molecule is obtained by the reaction of methyllithium with 1,1-Dibromo-2,2-bis(chloromethyl)cyclopropane:

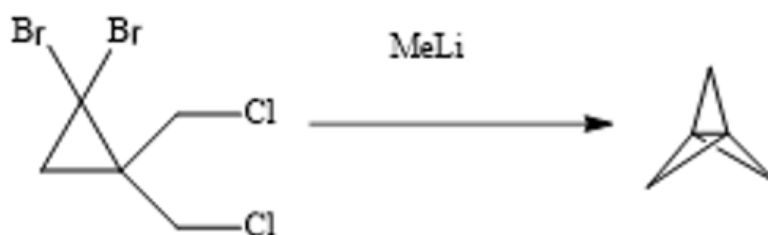


Figure 9. Synthesis of [1.1.1]propellane

When performing the BCP synthesis under radical condition, it is important to keep at minimum the formation of staffanes because its formation will inevitably lower the yield of the desired product. This compound is an oligomer originated by the reaction between the BCP radical and [1.1.1]propellane during the propagation step in radical chains. It is therefore important to develop reactions where the propellane attack by BCP radicals isn't energetic competitive with the formation of the product.



Figure 10. Staffane oligomer

## 3.2 Photocatalysis

Photocatalysis is defined as: “Change in the rate of a chemical reaction or its initiation under the action of ultraviolet, visible or infrared radiation in the presence of a substance (the Photocatalyst) that absorbs light and is involved in the chemical transformation of the reaction partners”. The photocatalyst (PC) is a molecular species (metal-based or a purely organic compound) that, once it absorbs light of the appropriate  $\lambda$  and reaches an electronically excited state, is capable of chemically modifying, at least, one of the reactants. Therefore, specific intermediates are formed that evolve towards the products through reaction pathways that are different from classical ground-state reactivity. The overall process finishes with the regeneration of the PC, which can start a new catalytic cycle with the absorption of another photon. The substrates can be activated through three different pathways, Photo-induced electron transfer (PET), Proton-coupled electron transfer (PCET) and Hydrogen-atom transfer (HAT), respectively.

### 3.2.1 Photo-induced electron transfer (PET) catalysis

In this process (also known as photoredox catalysis) the photocatalyst (PC), once photoexcited, can reduce or oxidize the substrate of interest through a single electron transfer (SET) event. The transition from the ground to the excited state leads to a substantial change in the electronic distribution of the PC for which the reduction/oxidation potentials in the excited state are totally different from the same potentials in the ground-state. Therefore, the excitation of the PC increases its reducing or oxidizing power.

### 3.2.2 Proton-coupled electron transfer (PCET) catalysis

In the case of multisite PCET, an electron and a proton arising from a single molecule are transferred to two different and independent acceptors, a Bronsted base and an oxidant (which may be an excited state PC), often through a concerted mechanism.

### 3.2.3 Hydrogen atom transfer (HAT) catalysis

Hydrogen-atom transfers reactions are key steps in a wide range of chemical and biochemical processes<sup>26</sup> in which a proton and an electron ( $e^- + H^+ = H$ ) from the same reactant are transferred in a single kinetic step to the same acceptor. Hydrogen-atom transfer is of pivotal importance in organic synthesis since it allows the selective activation of R-H bonds, and the reactivity can be tuned changing hydrogen abstractors, solvents etc.

### 3.2.4 Atom transfer radical addition (ATRA) process

In photocatalysis, numerous are the possible reaction pathways that the reactant can take once activated by the photocatalyst. Among these, one mechanism that frequently occurs in the field of photoredox catalysis is the atom transfer radical addition (ATRA) mechanism. The ATRA mechanism consists of the addition of a free radical species on a  $\pi$ -bond (alkene or alkyne) or to a strained molecule thus allowing the difunctionalization with the formation of two new  $\sigma$ -bonds C-C and C-X. This process is either capable of self-sustaining by being able to continue through a radical chain process requiring only an initiator to start or needs a photocatalyst.

## 4 Triethylborane-initiated reaction

The triethylborane-initiated reaction was the first reaction that ensured an easy access to halogenated BCPs without the use of harsh conditions. These compounds can be functionalized: lithiation resulted in an organolithium molecule that could react with electrophiles, transmetalation to the organozinc and cross-coupling with 2-bromopyridine gave pyridyl BCP and use of tris(trimethylsilyl)silane as hydrogen donor enabled deiodination of various BCP iodides.

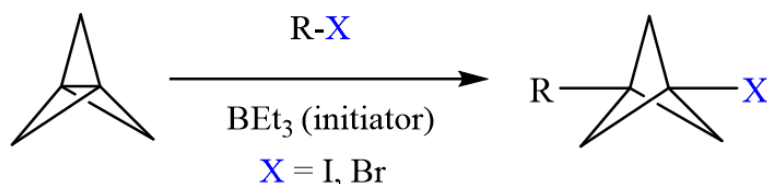


Figure 11. General reaction of [1.1.1]propellane with alkyl-halide in presence of an initiator

This reaction was first carried out using ethyl iodoacetate, optimal conditions were 1.1 equivalent of [1.1.1]propellane, 1 mol% of initiator, 0°C for 15 min in hexane, yield was 92%. Bromoacetate was converted partially and led to relevant staffane formation, instead 2-bromo-2-nitropropane yielded 67% using 1.3 equivalents of [1.1.1]propellane, 10 mol% of initiator, at room temperature for 15 min. This difference in reactivity is probably due to the more efficient bromine atom abstraction by the bicyclopentyl radical, which forms a more stable tertiary nitro-substituted radical. Alkyl iodides,  $\alpha$ -iodoketones, chloriodomethane, benzyl halides also showed good reactivity, amides and sulfones gave high yields<sup>10</sup>.

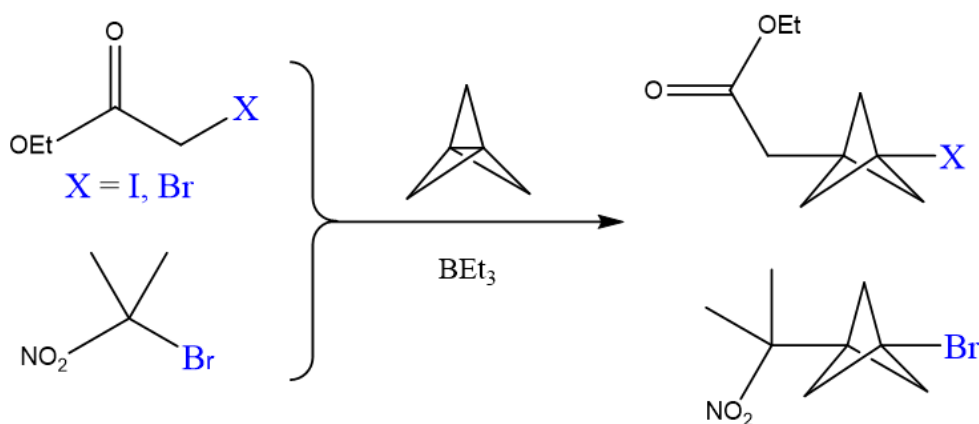


Figure 12. Functionalisation of [1.1.1]propellane using an initiator

### 4.1 Mechanism

The mechanism is that of an ATRA: the alkyl radical generated by the fragmentation of the carbon-halogen bond reacts with [1.1.1]propellane. The BCP radical thus generated reacts with the halogen radical giving the product. Theoretical studies explained that iodine atom abstraction and [1.1.1]propellane capture has lower activation barrier than the [1.1.1]propellane oligomerization. The bromine abstraction barrier energy was instead calculated to be similar to that of the staffane production, explaining the diverse reactivity of bromo and iodoacetate.<sup>10</sup>

## 5 Iridium photocatalyzed reaction

Although triethylborane initiated reaction works with simple 1-halo-3-substituted BCPs, they showed limited tolerance towards amines and aldehydes and were unable to access BCPs with aromatic substituents such as arenes and heteroarenes. *fac*-Ir(ppy)<sub>3</sub> catalyzed reactions do not have same problems and it is the first photoredox catalysis in carbon–carbon  $\sigma$ -bond functionalization. First trials started with Benzyl iodide and Pyridin iodide, optimal conditions are: 2 equivalents of [1.1.1]propellane, 2.5 mol% of PC, blue LEDs, *t*-BuCN as solvent and 87% yield.

This reaction was performed with a wide variety of compounds: heteroaromatic iodides, primary and secondary alkyl iodides, benzylic and heterobenzylic iodides, heterocyclic ketones and bicyclic products.

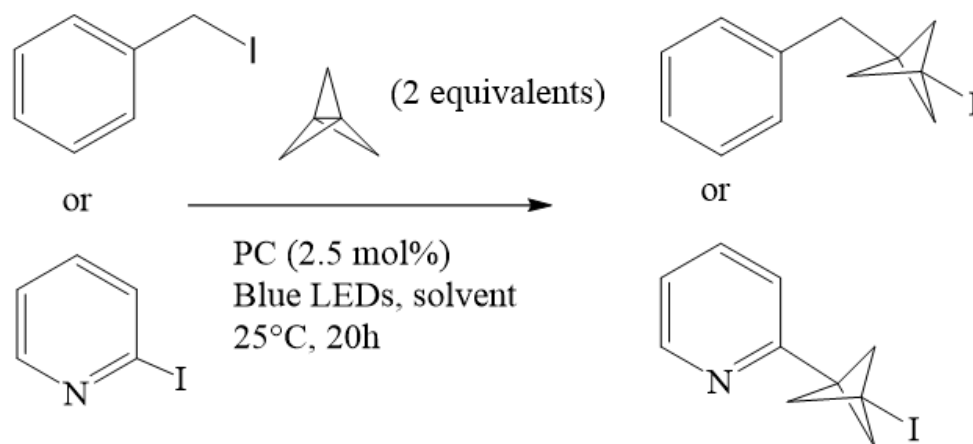


Figure 13. Iridium photocatalyzed functionalisation of [1.1.1]propellane

Quantum yield of some substrates was measured to understand the importance of the PC. In ethyl iodoacetate it was 682 out of 1000, meaning that this compound could undergo a propagation pathway to product without the presence of PC. 2-iodopyridine and *p*-CF<sub>3</sub>-benzyl iodide, instead had low QY values (7.4 and 1.4 respectively), revealing inefficient propagation and a resulting low yield under triethylborane-initiated ATRA. After these data it is clear the fundamental role of the PC in enabling additions of radicals not viable under classical radical chain conditions<sup>11</sup>.

## 5.1 Mechanism

The mechanism is that of a strain-release ATRA. After light excitation, an outer-sphere SET occur from the excited state Ir(III) complex to the halide substrate. This initiates the reductive cleavage of the carbon–halogen bond, giving a pyridine radical that induces strain-relief ring opening of [1.1.1]propellane, resulting in the formation of the BCP radical. Subsequently, this intermediate has two possible pathways: in Path a, it can undergo propagation to generate the product BCP and regenerate the chain carrier; alternatively, in Path b, it can undergo oxidative quenching by the Ir(IV) complex, regenerating the Ir(III) catalyst and forming the bicyclopentyl cation. The bicyclopentyl cation rapidly transforms into a cyclobutyl cation, which can be intercepted by iodide to produce cyclobutyl iodide. The founding of small quantities of cyclobutyl BCP iodide support this proposed mechanism. Presumably, this compound arises from a subsequent ATRA reaction of the cyclobutyl iodide<sup>11</sup>.

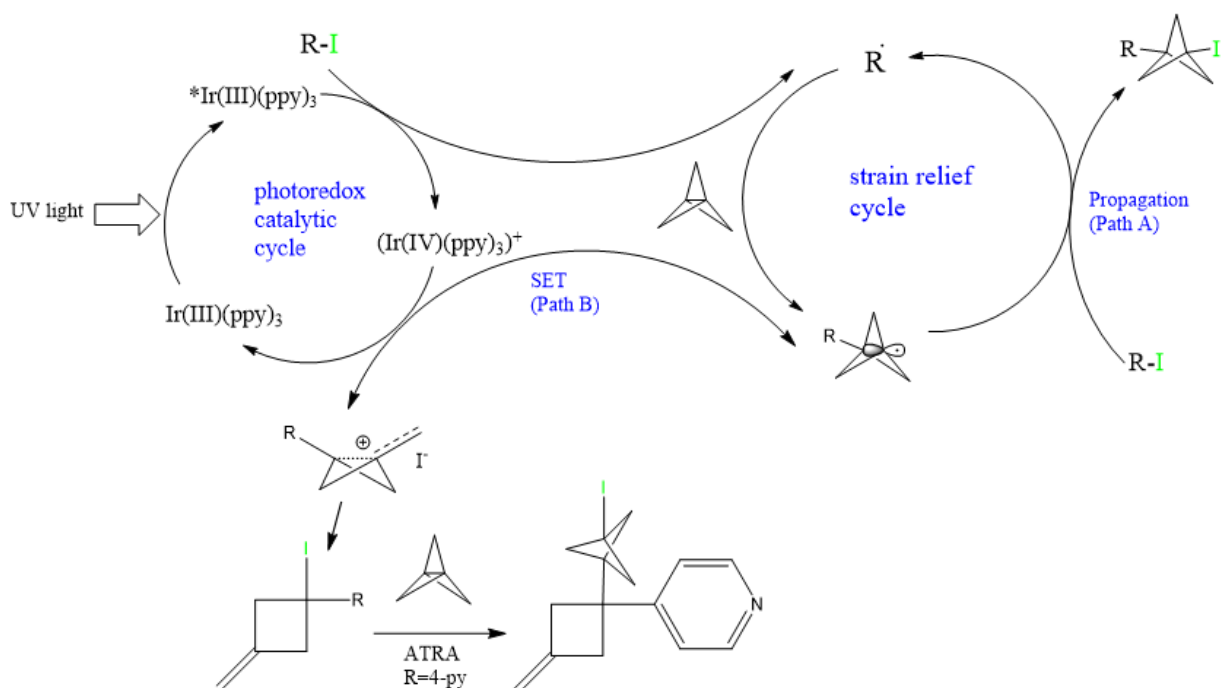


Figure 14. Mechanism of reaction

## 6 Organophotocatalyzed reactions

The more recent BCPs synthesis involves the use of organophotoredox catalyst. These catalysts are strongly reductive compound that can be modify to increase their efficiency and their general properties. They are easy to obtain and to functionalize and are of course free of transition metals. These aspects make them a great option to achieve sustainable, efficient and environmental safe synthesis of BCPs. The organophotocatalyst can bind through non-covalent interactions with the reagent generating an electron-donor complex (EDA). This complex will then participate to the radical-chain mechanism and therefore the synthesis of the BCP final compound.

### 6.1 EDA Complex

The electron-donor complex is a molecular aggregate originated from the union of an electron-rich molecule, acting as a Lewis base, and an electron-accepting molecules, acting as a Lewis acid. Their union form a new complex in the ground state, when it is excited by light with appropriate wavelength a single-electron-transfer can occur, generating radical intermediates. EDA complexes have been studied for since 1950 but only recently useful application in chemical synthesis have been found, an important aspect of their utility is the possibility of the EDA complex to absorb visible light, while perhaps the reagent alone wouldn't. In fact EDA complexes have new molecular orbitals, generated from the combination of frontier orbitals of reagent and the organophotocatalyst. This phenomenon is sometimes confirmed by the presence of a new charge-transfer band, attributable to a  $\Psi_{GS} \rightarrow \Psi_{ES}$  electronic transition. This electronic transition populates the excited state  $\Psi_{ES}$  and causes an intracomplex transfer from the donor, where usually lies the HOMO, to the acceptor where usually lies the LUMO. This generate a net charge separation in the complex and a radical ion pair in the acceptor. The energy needed to cause the HOMO-LUMO transition is proportional to the ionization potential of the donor and to the electron affinity of the acceptor, therefore comes in handy the use of cyclic voltammetry measurements to study the feasibility of an EDA complex. A problem that slowed down initially the use of photochemistry to form EDA complexes is the possibility that a back-electron-transfer (BET) could occur, restoring the ground state in an excited EDA complex, that obviously couldn't react. To prevent this event, is important to make the formation of the radical ion pair and the products kinetically competitive with the BET. A solution to achieve that is the use of leaving groups, wich irreversible fragmentation is rapid enough to compete with the BET. An important example is cleavage of carbon-halogen bonds, being irreversible and leading to the formation of the radical intermediate first and the product later instead of giving a BET.<sup>12</sup>

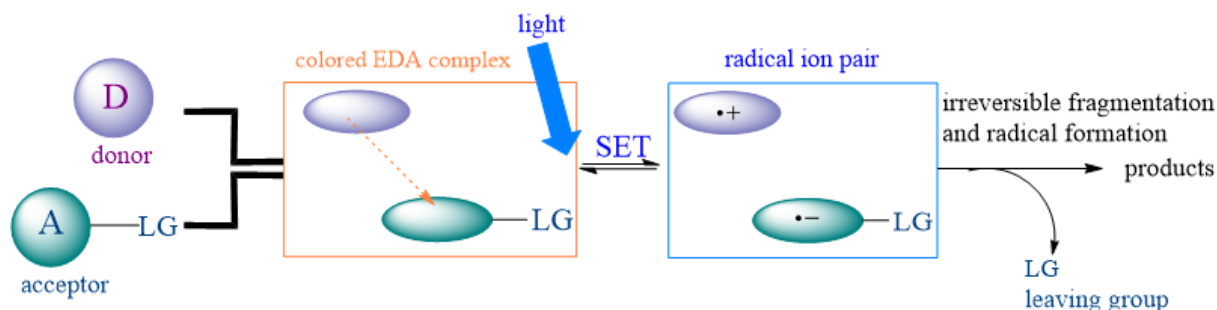


Figure 15. EDA complex scheme reaction



## 6.2 An hybrid bioisoster

Recently two organophotoredox routes have been developed to synthesize a particular functionalized BCPs, the difluoroalkyl BCP. There are numerous compounds and synthetic methods being developed in recent years to achieve BCPs functionalisation<sup>10,11,13-18</sup>, but they only stop at the replacement of benzene rings. Difluoroalkyl BCP is an hybrid bioisoster, i.e. comes from the union of two bioisosteres: BCPs and difluoromethylene, a motif used to replace ketones and oxygen atoms<sup>19,20</sup>. This new bioisoster offers the opportunity to substitute benzophenone cores present in several pharmaceutical<sup>21-26</sup>, or natural molecules<sup>21,27-29</sup> which possess important properties such as antifungal, anti-HIV, antimicrobial, antiviral, and antioxidant<sup>21</sup>. The use of BCPs has already been proved to be effective<sup>1-4</sup>, difluoromethylene too presents improved pharmacokinetic and pharmacodynamic profiles. For example in the Leukotriene A4 (LTA4) hydrolase inhibitor the substitution of ketone and ether group increased the drug potency ( $IC_{50}(\mu M) = 1.8$  ketone vs  $IC_{50}(\mu M) = 0.03$  ether vs  $IC_{50}(\mu M) = 0.011$  difluoromethylene)<sup>30,31</sup>. Difluoroalkyl BCP have also been installed in Adiporon, an adiponectin receptor agonist and it was found to be metabolically more stable than the original molecule, showing reduced clearance rates in human liver microsomes (HLM  $CL_{int} 362\mu L \cdot min^{-1}$  per mg protein in the substituted Adiporon vs HLM  $CL_{int} 532\mu L \cdot min^{-1}$  per mg protein in the original Adiporon)<sup>20</sup>.

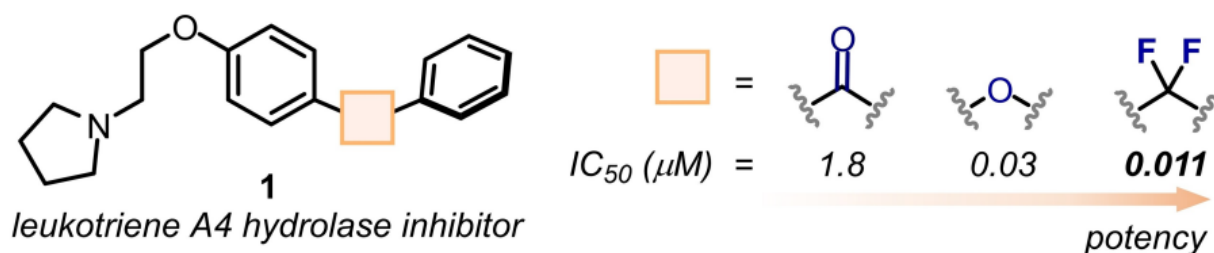


Figure 16. Bioisosteric replacement of leukotriene A4 hydrolase inhibitor with related enhanced potency

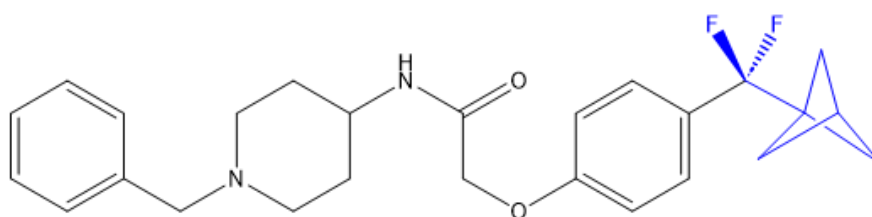


Figure 17. Hybrid bioisostere of Adiporon

### 6.3 Synthesis of difluoroalkyl BCP via ATRA

This reaction was first carried out with bromodifluoromethylphenylsulfone, this molecule was chosen for its easily removable sulfonyl moiety under reductive condition that could have given easy access to a difluoromethyl group. Several PC were used but the highest yield (89% after 1 hour of reaction and 96% after 2 hours) was found with 5 mol% of 12-aryl dihydrobenzoacridine (12ADBA) using Kessil lamp at 427nm and 45W, 1 equivalent of bromodifluoromethylphenylsulfone, 1 equivalent of [1.1.1]propellane at room temperature. This general reaction can be extent to produce 30 different bioactive molecules with yields up to 87% yield: alkyne, organolithium molecules followed by reaction with electrophiles, thioaryl, azoaryl and more. It could also be used to obtain BCPHep starting from [3.1.1]propellane<sup>30</sup>.

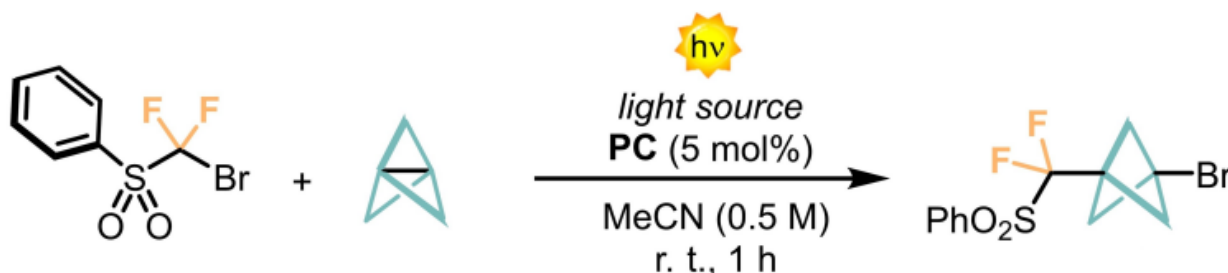


Figure 18. Synthesis of difluoroalkyl bicyclopentanes using organophotoredox catalyst

#### 6.3.1 Mechanism

The mechanism is that of an atom-transfer radical addition and start with the excitation of the EDA complex by visible light, a SET causes a net charge separation generating the intermediate III, following the cleavage of C-Br bond, and the PC's radical cation II. The intermediate III then attack the propellane through a strain-release reaction and generate the radical intermediate IV. This compound abstract a bromine atom from another bromodifluoromethylphenylsulfone molecule through a halogen atom transfer (XAT) process. The final product, difluoroalkylBCP is obtained and the intermediate III is regenerated. The PC's ground state is regenerated thanks to the reduction of the Br anion. The irreversible and rapid fragmentation of the C-Br bond deny the possibility of a BET. In fact, DFT studies confirmed that, after the SET happen, the C-Br bond length is 2.99 Å, making it almost entirely dissociated.

Analysis of the spin density map revealed the unpaired electron to be localized mostly on the difluoromethyl group, confirming this radical mechanism. The ATRA process is validated by the quantum yield (QY) being 1.1<sup>30</sup>.

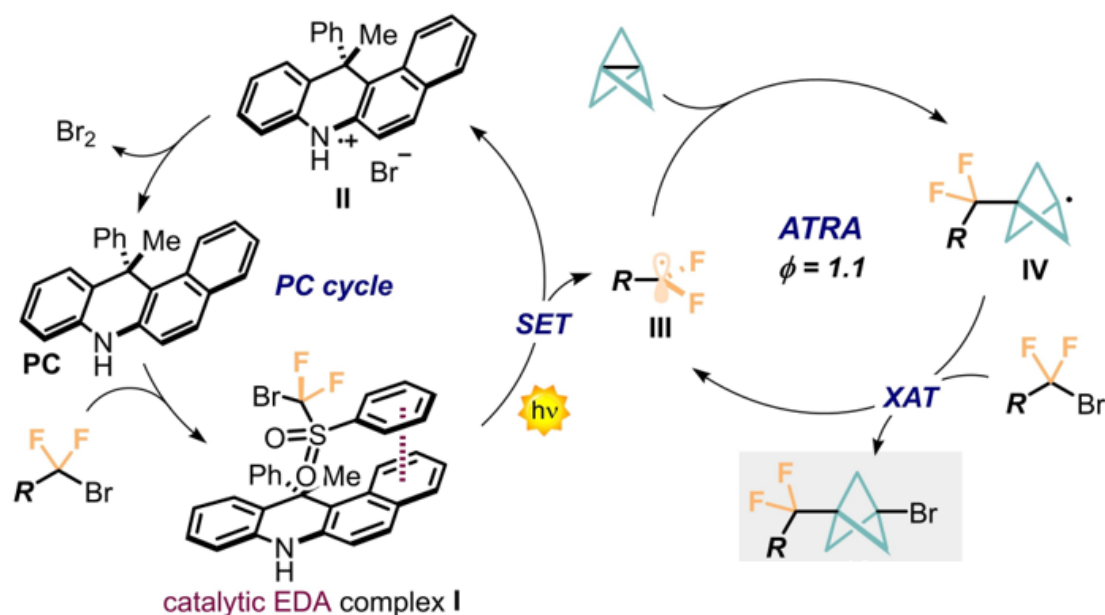


Figure 19. Proposed mechanism of reaction

### 6.3.2 Organophotocatalyst evaluation

Different PC were used but the one the reported the highest yield (89% after 1 hour of reaction and 96% after 2 hours) is the 12-aryl dihydrobenzoacridine (12ADBA).

The optical spectrum analysis showed that red-shifting was occurring when 12ADBA was added to the sulfone solution, this phenomenon was also confirmed to occur through TD-DFT calculations. That suggest the formation of and EDA complex between the photocatalyst and the reactant.

Spectroscopic and computational studies ruled out the possibility of an EDA complex created by H-bonds or halogen bonds, the most strong calculated interactions involved instead  $\pi$ - $\pi$  stacking between the aromatic motifs of sulfone and 12ADBA. Computational data provided interesting information about HOMO and LUMO locations within the complex, the first one mostly lean on the photocatalyst aromatic structure while the second one is mostly located on the sulfone<sup>30</sup>.

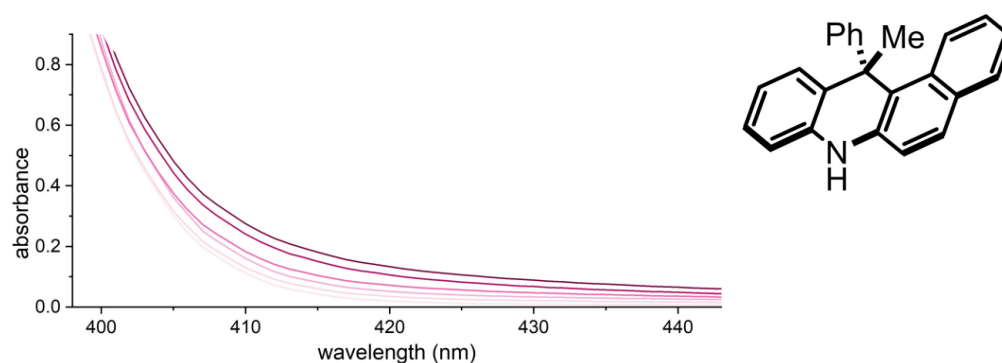


Figure 20. Red-shifting in the absorbance spectrum of sulfone with PC

### 6.3.3 12ADBA in-depth analysis

The 12ADBA derives from phenothiazine, one of the first PCs to be widely used. It has perhaps better features: it can be used to promote classical oxidative quenching or atom transfer radical polymerization, they can form an EDA complex with reactants and can be easily synthesized from common alkyne and diarylamine precursors.

Organic photocatalyst can access a Charge Transfer (CT) excited state if HOMO and LUMO orbitals are located on different molecule's zones. This is desirable because CT excited states possess more stable redox potentials and longer lifetimes.

Time dependent DFT calculations permitted to calculate HOMO and LUMO locations in the 12ADBA. The LUMO changed position in function of the R- functional group in the exocyclic aryl group. When R = H, OMe, or CF<sub>3</sub> it lies on the naphthalene within the PC's core, while if substituted with CN it is on the exocyclic ring. This different molecular orbital conformation will deeply influence the photochemical properties of the photocatalyst. Due to his additional benzene ring, the high conjugated  $\pi$  system permit a great visible-light absorption. Emission profiles of 5a-5c are very similar between each other, 5d instead is different, as suggested by the different LUMO location.

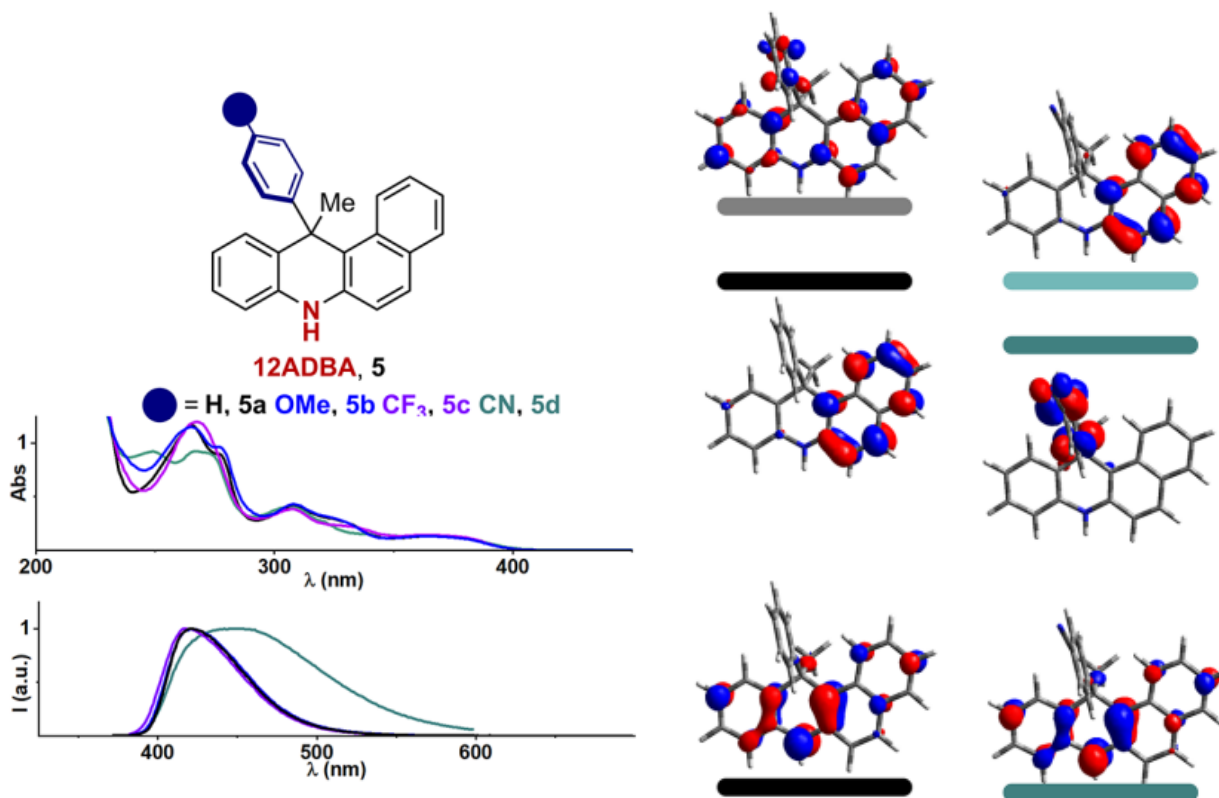


Figure 21. Absorbance spectrum of PC and HOMO and LUMO location within the molecule

To measure the redox potential of ground and excited state the photocatalyst has been analyzed through cyclic voltammetry. It was found a completely reversible behavior, that is a desirable aspect in PC. The presence of OMe- increased the HOMO energy by 0.3V, this short the HOMO-LUMO energy gap, favoring the single electron oxidation. All excited redox potential  $E^*_{ox}$  are highly negative.

To evaluate the ability of the photocatalyst to access CT excited state is important to measure the quantum yield (QY) and the excited state lifetime ( $\tau$ ). This PC shows a moderate and constant CT

character, retaining similar values of QY and  $\tau$  in scaffolds with different substituents, the only exception is the structure with CN, it has an increased stokes shift value of 81nm, a slightly longer lifetime of 9,4 ns and a decreased QY of 6%. These values clarify a better CT character in the CN substituent<sup>32</sup>.





●, PC	H, 5a	OMe, 5b	CF <sub>3</sub> , 5c	CN, 5d
E <sub>ox</sub> (V)	0.76	0.74	0.80	0.80
E* <sub>ox</sub> (V)	-2.37	-2.39	-2.34	-2.31
$\lambda_{\text{abs}}$ (nm)	364	363	364	362
$\lambda_{\text{em}}$ (nm)	420	421	420	443
E <sub>0,0</sub> (eV)	3.13	3.13	3.14	3.11
Stokes shift (nm)	56	58	56	81
QY (%)	30	26	29	6
$\tau$ (ns)	9.0	9.0	8.8	9.4
CT character				

Figure 22. Summarized values of PC characterization

#### 6.4 Synthesis of aryl difluoromethyl BCP

This reaction involves the presence of [1.1.1]propellane,  $\gamma$ -terpinene as hydrogen atom donor and trifluoromethylarenes, an easy commercially available compound. Optimal conditions require 1.2 equivalents of the base Cs<sub>2</sub>CO<sub>3</sub>, DMSO as solvent, room temperature for 12 hours, 10mol% of PC, 5.0 equivalents of  $\gamma$ -terpinene and the yield is 74%, with a 15% production of staffane.

This reaction is also compatible with different electron-donating and electron-withdrawing substituents with yields between 30 and 74% such as: amides, ethers, anilines, unprotected amines, alcohols and heterocycles as pyridine. Instead of using of [1.1.1]propellane, [3.1.1]propellane can be employed to obtain BCPHep. The difluoromethyl bicycloalkane boronate can also be synthesized in a three-component coupling, the Bpin group functionalization can be used to obtain alcohols or organotrifluoroborate salts, these salts can be later transformed in further useful functional groups<sup>20</sup>.

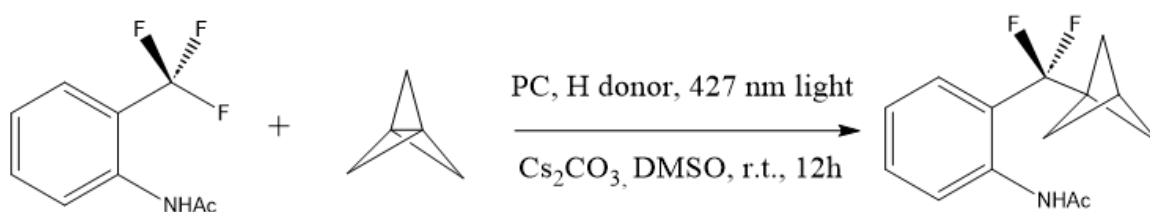


Figure 23. General synthesis of aryl difluoromethyl BCP

### 6.4.1 Mechanism

The excitation of the PN(I) anionic catalyst through visible-light leads to the formation of a highly reducing excited state II. The subsequent single-electron transfer to the trifluoromethylarene results in the generation of the corresponding difluorobenzyl radical. This radical is efficiently trapped by [1.1.1]propellane, leading to the formation of the BCP radical. This radical intermediate then selectively abstracts a hydrogen atom from  $\gamma$ -terpinene, facilitating the production of the desired BCP product and the cyclohexadienyl radical. To complete the catalytic cycle, a single electron transfer occurs between the de-hydrogenated radical  $\gamma$ -terpinene and the oxidized photocatalyst III, regenerating the initial photocatalyst I<sup>20</sup>.

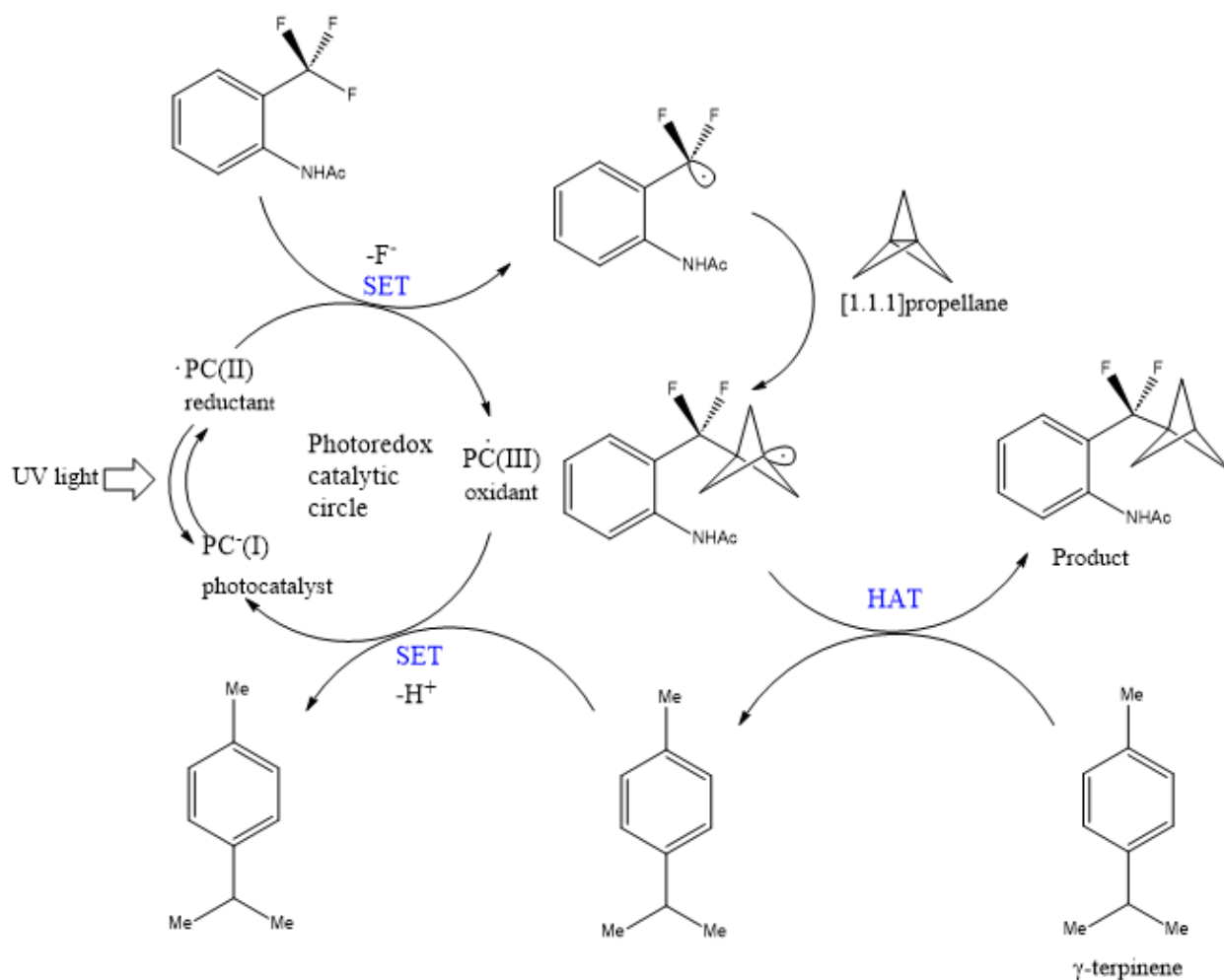


Figure 24. Mechanism of reaction

### 6.4.2 Organophotocatalyst evaluation

The PC screening started with trials of N-phenylphenothiazine and phosphinophenolate showing moderate yields (respectively 36% and 43%), even iridium based catalyst fac-Ir(ppy)<sub>3</sub> was used but reported low yield (6%). Then the phosphine group was installed on arylamine to facilitate photo-induced electron transfer processes since other studies reported it would lead to triplet state, which possess longer lifetime. After some functionalization, the carbazole-based catalyst was found to be the one with highest performances ( $E_{1/2}^{\text{red}} [*PN -/PN \cdot] = -3.26 \text{ V}$  vs. the saturated calomel electrode in DMSO) and yield (74%). Since PC without ortho-PPh<sub>2</sub> substitution and N-anionic motif reported low or 0% yields, it is plausible that both these groups are crucial for the photocatalytic reactivity<sup>20</sup>.

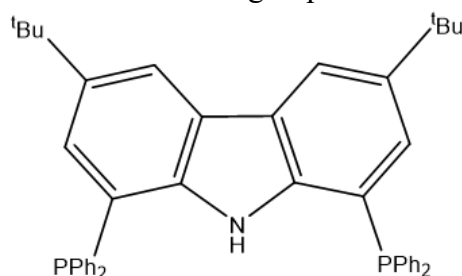


Figure 25. Carbazole-based PC

## 7 Conclusions

BCP is a saturated and 3D shaped molecule that can serve as a mono and *para* substituted benzene bioisostere. This substitution is possible due to their similar C-C bond length (2.82Å in benzene and 1.85Å in BCP) and their identical coplanar orientation of substituents. BCP possess better properties than benzene: an increased solubility due to lack of  $\pi$ -stacking between aromatic rings, an increased metabolic stability, thus in pharmaceuticals it has similar or in some cases greater potency.

BCP is obtained from [1.1.1]propellane. This molecule has a unique chemistry and can undergo both nucleophilic, electrophilic and radical attacks due to his pliable orbital structure. Especially radical addition are being developed in recent years to access BCPs. In the beginning only harsh conditions were known but they had low compatibility with functional groups, then triethylborane initiated reactions slightly improved this aspect, despite retaining incompatibility with amines, aldehydes and aromatic substituents such as arenes and heteroarenes. Although that they remain a valuable option to synthesize simple compounds with yields up to 92%.

Iridium catalyzed reaction did not have such problems with functional groups, used a commercially available catalyst and permitted to obtain a large variety of compounds, especially those which could not undergo self-sustained radical chain propagation.

Organophotocatalyzed reactions besides having all the just listed benefits, were a more sustainable option, not implying the presence of transition metals. OrganoPC can form with substrate an EDA complex that if excited will facilitate the SET to the compound. The CT excited state where HOMO and LUMO are located in different zones of the PC is desirable because has longer lifetime and more stable redox potential. In 12ADBA functionalization the CN-phenil-substitued molecule had the most CT character.

All these reactions start with the generation of a radical specie that then implement the shell-opening of [1.1.1]propellane generating a BCP radical that abstract from another molecule an halogen atom, an hydrogen atom or a boron atom. Usually the mechanism follow an ATRA chain, self sustained if possible or photocatalyzed. These reported synthetic methods combined grant access to a wide variety of BCP molecules.

## 8 Bibliography

- (1) Denisenko, A.; Garbuz, P.; Shishkina, S. V.; Voloshchuk, N. M.; Mykhailiuk, P. K. Saturated Bioisosteres of *Ortho*-Substituted Benzenes. *Angewandte Chemie* **2020**, *132* (46), 20696–20702. <https://doi.org/10.1002/ange.202004183>.
- (2) Frank, N.; Nugent, J.; Shire, B. R.; Pickford, H. D.; Rabe, P.; Sterling, A. J.; Zarganes-Tzitzikas, T.; Grimes, T.; Thompson, A. L.; Smith, R. C.; Schofield, C. J.; Brennan, P. E.; Duarte, F.; Anderson, E. A. Synthesis of Meta-Substituted Arene Bioisosteres from [3.1.1]Propellane. *Nature* **2022**, *611* (7937), 721–726. <https://doi.org/10.1038/s41586-022-05290-z>.
- (3) Mykhailiuk, P. K. Saturated Bioisosteres of Benzene: Where to Go Next? *Org. Biomol. Chem.* **2019**, *17* (11), 2839–2849. <https://doi.org/10.1039/C8OB02812E>.
- (4) Stepan, A. F.; Subramanyam, C.; Efremov, I. V.; Dutra, J. K.; O’Sullivan, T. J.; DiRico, K. J.; McDonald, W. S.; Won, A.; Dorff, P. H.; Nolan, C. E.; Becker, S. L.; Pustilnik, L. R.; Riddell, D. R.; Kauffman, G. W.; Kormos, B. L.; Zhang, L.; Lu, Y.; Capetta, S. H.; Green, M. E.; Karki, K.; Sibley, E.; Atchison, K. P.; Hallgren, A. J.; Oborski, C. E.; Robshaw, A. E.; Sneed, B.; O’Donnell, C. J. Application of the Bicyclo[1.1.1]Pentane Motif as a Nonclassical Phenyl Ring Bioisostere in the Design of a Potent and Orally Active  $\gamma$ -Secretase Inhibitor. *J. Med. Chem.* **2012**, *55* (7), 3414–3424. <https://doi.org/10.1021/jm300094u>.
- (5) Bellotti, P.; Glorius, F. Strain-Release Photocatalysis. *J. Am. Chem. Soc.* **2023**, *145* (38), 20716–20732. <https://doi.org/10.1021/jacs.3c08206>.
- (6) Sterling, A. J.; Dürr, A. B.; Smith, R. C.; Anderson, E. A.; Duarte, F. Rationalizing the Diverse Reactivity of [1.1.1]Propellane through  $\sigma$ - $\pi$ -Delocalization. *Chem. Sci.* **2020**, *11* (19), 4895–4903. <https://doi.org/10.1039/D0SC01386B>.
- (7) Wiberg, K. B.; Waddell, S. T. Reactions of [1.1.1]Propellane. *J. Am. Chem. Soc.* **1990**, *112* (6), 2194–2216. <https://doi.org/10.1021/ja00162a022>.
- (8) Kaszynski, P.; McMurdie, N. D.; Michl, J. Synthesis of Doubly Bridgehead Substituted Bicyclo[1.1.1]Pentanes. Radical Transformations of Bridgehead Halides and Carboxylic Acids. *J. Org. Chem.* **1991**, *56* (1), 307–316. <https://doi.org/10.1021/jo00001a058>.
- (9) Eur J Org Chem - April 2000 - Messner - Nickel- and Palladium-Catalyzed Cross-Coupling Reactions at the Bridgehead of.Pdf.
- (10) Caputo, D. F. J.; Arroniz, C.; Dürr, A. B.; Mousseau, J. J.; Stepan, A. F.; Mansfield, S. J.; Anderson, E. A. Synthesis and Applications of Highly Functionalized 1-Halo-3-Substituted Bicyclo[1.1.1]Pentanes. *Chem. Sci.* **2018**, *9* (23), 5295–5300. <https://doi.org/10.1039/C8SC01355A>.
- (11) Nugent, J.; Arroniz, C.; Shire, B. R.; Sterling, A. J.; Pickford, H. D.; Wong, M. L. J.; Mansfield, S. J.; Caputo, D. F. J.; Owen, B.; Mousseau, J. J.; Duarte, F.; Anderson, E. A. A General Route to Bicyclo[1.1.1]Pentanes through Photoredox Catalysis. *ACS Catal.* **2019**, *9* (10), 9568–9574. <https://doi.org/10.1021/acscatal.9b03190>.
- (12) Crisenza, G. E. M.; Mazzarella, D.; Melchiorre, P. Synthetic Methods Driven by the Photoactivity of Electron Donor–Acceptor Complexes. *J. Am. Chem. Soc.* **2020**, *142* (12), 5461–5476. <https://doi.org/10.1021/jacs.0c01416>.
- (13) Gupta, S.; Srinivasu, V.; Sureshkumar, D. Metal and Catalyst-Free Strategy to Access 1,3-Thio-Heteroaryl BCP Derivatives. *Org. Biomol. Chem.* **2023**, *21* (40), 8136–8140. <https://doi.org/10.1039/D3OB01377D>.



- (14) Srinivasu, V.; Das, D.; Chandu, P.; Ghosh, K. G.; Sureshkumar, D. Metal-Free Photoredox Four-Component Strategy to 1,3-Functionalized BCP Derivatives. *Org. Lett.* **2023**, *25* (28), 5308–5313. <https://doi.org/10.1021/acs.orglett.3c01877>.
- (15) Garry, O. L.; Heilmann, M.; Chen, J.; Liang, Y.; Zhang, X.; Ma, X.; Yeung, C. S.; Bennett, D. J.; MacMillan, D. W. C. Rapid Access to 2-Substituted Bicyclo[1.1.1]Pentanes.
- (16) Yan, B.; Xu, G.; Han, H.; Hong, J.; Xu, W.; Lan, D.; Yu, C.; Jiang, X. Synthesis of 1-Perfluoroalkyl-3-Heteroaryl Bicyclo[1.1.1]Pentanes *via* Visible Light-Induced and Metal-Free Perfluoroalkylation of [1.1.1]Propellane. *Green Chem.* **2023**, *25* (5), 1948–1954. <https://doi.org/10.1039/D2GC04683K>.
- (17) Zhu, H.; Wu, S.; Zhu, B.; Li, J.; Lan, D.; Xu, W.; Xu, G.; Zhu, Y.; Yu, C.; Jiang, X. Visible Light-Induced *Gem*-Difluoroallylation of [1.1.1]Propellane to Access *Gem*-Difluoroallylic Bicyclo[1.1.1]Pentanes. *Chem. Commun.* **2023**, *59* (35), 5213–5216. <https://doi.org/10.1039/D3CC00822C>.
- (18) Gao, Y.; Zheng, Z.; Zhu, Y.; Xu, W.; Zhou, Y.; Yu, C.; Jiang, X. Visible Light-Induced Synthesis of 1,3-Disubstituted Bicyclo[1.1.1]Pentane Ketones *via* Cooperative Photoredox and N-Heterocyclic Carbene Catalysis. *Green Chem.* **2023**, *25* (10), 3909–3915. <https://doi.org/10.1039/D3GC00643C>.
- (19) Meanwell, N. A. Fluorine and Fluorinated Motifs in the Design and Application of Bioisosteres for Drug Design. *J. Med. Chem.* **2018**, *61* (14), 5822–5880. <https://doi.org/10.1021/acs.jmedchem.7b01788>.
- (20) Chen, M.; Cui, Y.; Chen, X.; Shang, R.; Zhang, X. *C–F Bond Activation Enables Synthesis of Aryl Difluoromethyl Bicyclopentanes as Benzophenone-Type Bioisosteres*; preprint; Chemistry, 2023. <https://doi.org/10.26434/chemrxiv-2023-wd932>.
- (21) Surana, K.; Chaudhary, B.; Diwaker, M.; Sharma, S. Benzophenone: A Ubiquitous Scaffold in Medicinal Chemistry. *Med. Chem. Commun.* **2018**, *9* (11), 1803–1817. <https://doi.org/10.1039/C8MD00300A>.
- (22) Wang, G.; Liu, W.; Tang, J.; Ma, X.; Gong, Z.; Huang, Y.; Li, Y.; Peng, Z. Design, Synthesis, and Anticancer Evaluation of Benzophenone Derivatives Bearing Naphthalene Moiety as Novel Tubulin Polymerization Inhibitors. *Bioorganic Chemistry* **2020**, *104*, 104265. <https://doi.org/10.1016/j.bioorg.2020.104265>.
- (23) Lakshmi Ranganatha, V.; Zameer, F.; Meghashri, S.; Rekha, N. D.; Girish, V.; Gurupadaswamy, H. D.; Khanum, S. A. Design, Synthesis, and Anticancer Properties of Novel Benzophenone-Conjugated Coumarin Analogs. *Archiv der Pharmazie* **2013**, *346* (12), 901–911. <https://doi.org/10.1002/ardp.201300298>.
- (24) Jabeen, I.; Pleban, K.; Rinner, U.; Chiba, P.; Ecker, G. F. Structure–Activity Relationships, Ligand Efficiency, and Lipophilic Efficiency Profiles of Benzophenone-Type Inhibitors of the Multidrug Transporter P-Glycoprotein. *J. Med. Chem.* **2012**, *55* (7), 3261–3273. <https://doi.org/10.1021/jm201705f>.
- (25) Khanum, S. A.; Shashikanth, S.; Deepak, A. V. Synthesis and Anti-Inflammatory Activity of Benzophenone Analogues. *Bioorganic Chemistry* **2004**, *32* (4), 211–222. <https://doi.org/10.1016/j.bioorg.2004.04.003>.
- (26) Venu, T. D.; Shashikanth, S.; Khanum, S. A.; Naveen, S.; Firdouse, A.; Sridhar, M. A.; Shashidhara Prasad, J. Synthesis and Crystallographic Analysis of Benzophenone Derivatives—The Potential Anti-Inflammatory Agents. *Bioorganic & Medicinal Chemistry* **2007**, *15* (10), 3505–3514. <https://doi.org/10.1016/j.bmc.2007.02.051>.
- (27) Acuna, U.; Jancovski, N.; Kennelly, E. Polyisoprenylated Benzophenones from Clusiaceae: Potential Drugs and Lead Compounds. *CTMC* **2009**, *9* (16), 1560–1580. <https://doi.org/10.2174/156802609789909830>.

- (28) Wu, S.-B.; Long, C.; Kennelly, E. J. Structural Diversity and Bioactivities of Natural Benzophenones. *Nat. Prod. Rep.* **2014**, *31* (9), 1158–1174. <https://doi.org/10.1039/C4NP00027G>.
- (29) Kumar, S.; Sharma, S.; Chattopadhyay, S. K. The Potential Health Benefit of Polyisoprenylated Benzophenones from *Garcinia* and Related Genera: Ethnobotanical and Therapeutic Importance. *Fitoterapia* **2013**, *89*, 86–125. <https://doi.org/10.1016/j.fitote.2013.05.010>.
- (30) Cuadros, S.; Goti, G.; Barison, G.; Rauli, A.; Bortolato, T.; Pelosi, G.; Costa, P.; Dell'Amico, L. A General Organophotoredox Strategy to Difluoroalkyl Bicycloalkane (CF<sub>2</sub>-BCA) Hybrid Bioisosteres\*\*. *Angewandte Chemie* **2023**, *135* (31), e202303585. <https://doi.org/10.1002/ange.202303585>.
- (31) Penning, T. D.; Chandrakumar, N. S.; Chen, B. B.; Chen, H. Y.; Desai, B. N.; Djuric, S. W.; Docter, S. H.; Gasiiecki, A. F.; Haack, R. A.; Miyashiro, J. M.; Russell, M. A.; Yu, S. S.; Corley, D. G.; Durley, R. C.; Kilpatrick, B. F.; Parnas, B. L.; Askonas, L. J.; Gierse, J. K.; Harding, E. I.; Highkin, M. K.; Kachur, J. F.; Kim, S. H.; Krivi, G. G.; Villani-Price, D.; Pyla, E. Y.; Smith, W. G.; Ghoreishi-Haack, N. S. Structure–Activity Relationship Studies on 1-[2-(4-Phenylphenoxy)Ethyl]Pyrrolidine (SC-22716), a Potent Inhibitor of Leukotriene A<sub>4</sub> (LTA<sub>4</sub>) Hydrolase. *J. Med. Chem.* **2000**, *43* (4), 721–735. <https://doi.org/10.1021/jm990496z>.
- (32) Bortolato, T.; Simionato, G.; Vayer, M.; Rosso, C.; Paoloni, L.; Benetti, E. M.; Sartorel, A.; Lebœuf, D.; Dell'Amico, L. The Rational Design of Reducing Organophotoredox Catalysts Unlocks Proton-Coupled Electron-Transfer and Atom Transfer Radical Polymerization Mechanisms. *J. Am. Chem. Soc.* **2023**, *145* (3), 1835–1846. <https://doi.org/10.1021/jacs.2c11364>.